This letter has been accepted for publication in the IEEE Communications Letters on Oct 2016.

Upper Bound Analysis of the Handover Performance in HetNets

Irene Pappalardo Andrea Zanella Michele Zorzi

***Abstract*—Handover in HetNets is an interesting research challenge that has attracted considerable attention in recent years, producing a variety of handover schemes that are difficult to compare because they differ in the considered assumptions and target user/network utility functions. Therefore, how much room is left for further optimization is quite unclear. In this letter, we propose a framework to derive an upper bound for the performance of handover in HetNets that can be used as a benchmark to compare different practical handover schemes. The approach computes the optimal handover strategy as a function of the user's speed, cell size and load conditions, under the ideal assumption of non-causal knowledge of the channels from terminal and base stations. The proposed framework is then used to provide a comparative performance analysis among some existing handover schemes.**

I. Introduction

Handover (HO) is the process that allows a mobile User Equipment (UE) to change its serving base station (BS) to maintain a sufficient service level. In classic cellular systems, consisting of macro cells of approximately equal size, the HO process is typically driven by the Reference Signal Received Power (RSRP) from the different BSs. Such a simple strategy, however, is no longer efficient in a Heterogeneous Network (HetNet) scenario, where small cells (micro, pico and femto cells) can be densely deployed within the coverage area of macro cells and cell loads can vary widely. In this scenario, it is hence important to enhance the HO strategy with *context-awareness*, e.g., accounting for the size and traffic load of the serving and surrounding cells, the UE speed and mobility pattern, and so on [1], [2].

The recent literature indeed reports a number of different HO strategies for HetNets embodying different levels of context-awareness, and targeting different key performance indices, such as power consumption for a given minimum Signal To Interference and Noise Ratio (SINR) [3], energy consumption and interference at the UE side [4], network capacity under user fairness constraints [5], or congestion level of the different cells [6]–[8]. The different assumptions and target metrics considered in these works, however, make it rather difficult to compare the various HO algorithms and to assess the residual margin for further improvements [9].

Motivated by these considerations, in this letter we propose a mathematical framework that makes it possible to derive an *upper bound for the HO performance* under the assumption that the position of the Base Stations (BSs), the UE trajectory, and the channel parameters are known in advance. This bound can hence be used as a benchmark to compare the performance of different practical algorithms and assess the remaining room for improvement. Hence, the scope of this letter is *not* to present a new handover algorithm, but rather a general framework to compute the performance upper bound of any HO algorithm.[1] To illustrate the potential of the proposed model, we present a performance comparison of three different HO policies taken from [10]–[12], and assess their distance from the bound. In this case-study we focus on the average Shannon capacity experienced by a mobile UE along its trajectory, but the model is general enough to accommodate different context parameters and performance indices.

II. System Model and Optimal Handover Policy

The addressed scenario consists of a set $\{B_0, B_1, \ldots, B_N\}$ of BSs, whose locations are assumed to be known. We then target a mobile UE that crosses the area along a predetermined trajectory. We denote by $\Gamma_i(\mathbf{a}, t)$ the RSRP that the UE collected from B_i at time t, when it was in position $\mathbf{a}$ along the trajectory. Assuming a pathloss plus fading propagation model, in the downlink channel we then have $\Gamma_i(\mathbf{a}, t) = \Gamma_i^{tx} g_i(\mathbf{a}) \alpha_i(t),\ i \in \{0, \ldots, N\}$, where Γ_i^{tx} is the transmit power of B_i, $g_i(\mathbf{a})$ is the pathloss from B_i to point $\mathbf{a}$, which is assumed known, and $\alpha_i(t)$ is the fast-fading channel gain at time t that, instead, is assumed unknown.[2] We can hence determine the average performance experienced by the UE when crossing the area, for a given HO strategy.

For analytical tractability, it is convenient to consider a discrete version of the problem that is obtained by sampling the process $\Gamma_i(\mathbf{a}, t)$ with a time step T_c long enough to break the correlation between fading samples. For instance, for a given UE speed v, and assuming Rayleigh fading, the sampling interval can be set equal to the channel coherence time, which is given by (see [13]) $T_c = \sqrt{9/(16\pi)c^2/(vf_c)}$ where c is the speed of light and f_c is the carrier frequency.

The sampling period in the time dimension corresponds to a constant sampling distance along the trajectory, whose length $\Delta_c = vT_c = \sqrt{9/(16\pi)c^2/f_c}$ can be interpreted as a *coherence space*. The sampled version of the RSRP process, hence, can be written as

$$\Gamma_i(\mathbf{a}_k, \tau_k) = \Gamma_i^{tx} g_i(\mathbf{a}_k) \alpha_i(\tau_k)\,, \tag{1}$$

where $\mathbf{a}_k$ and τ_k are the kth sampling points along the UE trajectory and in time, respectively. Assuming the UE is served by B_i at this sampling point, the Signal-to-Interference-Ratio[3] (SIR) experienced by the UE can be expressed as

$$\gamma_i(\mathbf{a}_k, \tau_k) = \frac{\Gamma_i(\mathbf{a}_k, \tau_k)}{\sum_{j \neq i} \Gamma_j(\mathbf{a}_k, \tau_k)}\,. \tag{2}$$

At each point along its trajectory, the UE can either be served by a certain BS, or perform a HO towards another

[1] Note that the bound is indeed achievable if the network topology, UE mobility pattern, and channel states are known.

[2] The proposed framework can also be used to determine the achievable HO performance under exact and non-causal knowledge of the whole channel gain along the trajectory, as done at the end of this letter.

[3] Assuming the system is interference-limited, the noise term is neglected.

BS. We assume that the HO process takes a time T_H to be concluded, corresponding to a certain number $h = \lceil vT_H/\Delta_c \rceil$ of spatial sampling intervals, and that during this time the UE is not served by any BS. Note that the higher the speed v of the UE, the larger the number of steps spent in this transition state.[4] We hence denote by $\mathcal{B}_i$ the state of the UE when it is connected to B_i, while $\mathcal{H}_j^\ell$ indicates that the UE is at the ℓth step of the HO procedure to connect to B_j. The set of all possible states is then denoted as[5] $\Omega = \mathcal{B} \cup \mathcal{H}$, where $\mathcal{B} = \{\mathcal{B}_i\}_{i=0,\dots,N}$ and $\mathcal{H} = \{\mathcal{H}_j^\ell\}_{j=0,\dots,N}^{\ell=1,\dots,h}$.

Denoting by K the total number of sample points along the UE trajectory, any HO strategy can be represented by a vector of K elements, $S = [s(1), \dots, s(K)]$, where $s(i) \in \Omega$ represents the state of the UE at the ith sample point. The objective, hence, is to find the policy S^* that maximizes a certain utility function over all the K points along the trajectory followed by the UE.

If the utility function can be expressed as the sum of the utility experienced by the UE at each point along the trajectory, then the optimization problem can be solved using a simple adaptation of the Viterbi algorithm. Let $\boldsymbol{\pi}_s \subset \Omega$ be the set of states from which the UE can reach state $s \in \Omega$ in one step. We have

$$\boldsymbol{\pi}_s = \begin{cases} \{s\} \cup \{\mathcal{H}_s^h\} & , \quad s \in \mathcal{B}\,; \\ \mathcal{B} \setminus \{\mathcal{B}_j\} & , \quad s = \mathcal{H}_j^1\,; \\ \{\mathcal{H}_j^{\ell-1}\} & , \quad s = \mathcal{H}_j^\ell\,,\ \ell \neq 1\,; \end{cases} \tag{3}$$

where the first row says that the UE can be connected to BS B_s only if it was already connected to the same BS at the previous step or it just completed the handover process towards that BS, the second row indicates that the UE will never start a HO process towards the same BS it is already connected to, while the third row states that, once started, the HO process continues for exactly h steps. We can then build a trellis diagram of depth K, where every step $k = 1, \dots, K$ corresponds to a sample along the UE trajectory, and where state q at step $k+1$ can only be reached from a state $p \in \boldsymbol{\pi}_q$ at step k.[6]

Now, each link of the trellis that ends into state s at step k is assigned a certain *gain* $C_s(k)$, which only depends on the arrival state s. Following the rules of the Viterbi algorithm, and assuming the initial state of the UE is $s_0 \in \Omega$, the utility function at every step k can be expressed recursively as follows:

$$\mathcal{U}_s(k) = \max_{q \in \boldsymbol{\pi}_s} \mathcal{U}_q(k-1) + C_s(k)\,,\ \forall s \in \Omega,\ k = 1, \dots, K\,, \tag{4}$$

with $U_{s_0}(0) = C_{s_0}(0)$ and $U_s(0) = 0$ for any $s \neq s_0$. Once the utility function is computed for all the possible states along the trellis, the optimal policy is obtained by starting from

$$s^*(K) = \arg \max_{s \in \Omega} \mathcal{U}_s(K)\,, \tag{5}$$

[4]The model can accommodate different values of T_H for each serving BS, though for ease of presentation here we assume T_H to be a common constant.

[5]The symbols $\cup$ and $\setminus$ denote the set union and the set theoretic difference operations.

[6]While the trellis of the standard Viterbi algorithm is fully connected at every step, the precedence rules expressed in (3) make it possible to reduce the complexity of the algorithm from $\mathcal{O}(K(N+1)^2h^2)$ to $\mathcal{O}(K(N+1)(N+1+h))$. We remark also that the complexity can be further reduced by considering only the handover processes among neighboring cells.

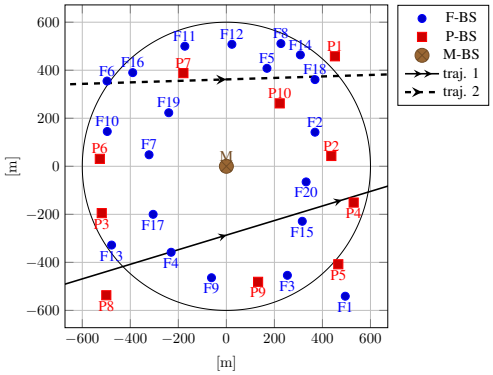

Fig. 1: Reference heterogeneous scenario.

and going backward along the path that maximizes the utility at each step, i.e.,

$$s^*(k) = \arg \max_{q \in \boldsymbol{\pi}_{s^*(k+1)}} \mathcal{U}_q(k)\,,\ k = K-1, \dots, 1\,. \tag{6}$$

Note that the computation of the optimal policy S^* requires the non-causal (anticipatory) knowledge of the gain $C_s(k)$ for any step k and any state s, a condition hardly met in practice. For this reason, the performance attained by S^* represents an upper bound for any practical HO algorithm where such non-causal knowledge is not available, thereby providing a useful benchmark.

III. Performance Evaluation

In this section, we compare the performance achieved in a given scenario by some practical HO algorithms proposed in the literature, and assess their gap with respect to the optimal HO performance obtained with the proposed model in the same scenario.

A. Optimal performance analysis

We consider the case of a single macro cell, containing N small-cell BSs. We assume that the target UE follows a straight trajectory at constant speed v, and that the RSRPs are affected by Rayleigh fading, so that the coefficients $\alpha_i(t)$ are exponential random variables with unit mean. The utility function is the average Shannon capacity experienced by the UE along its trajectory. Hence, the gain in state s at time k is given by

$$C_s(k) = \begin{cases} \lambda_s \mathbb{E}\left[\log_2\left(1 + \gamma_s(\mathbf{a}_k, \tau_k)\right)\right] & , \quad s \in \mathcal{B}\,; \\ 0 & , \quad s \in \mathcal{H}\,; \end{cases} \tag{7}$$

where $\gamma_s(\mathbf{a}_k, \tau_k)$ is defined in (2), while $\lambda_s \in [0,1]$ is the available fraction of the cell capacity. Note that we assume zero capacity during handover, in order to reflect the performance loss incurred by the UE when switching BS. Furthermore, the gain can be set to zero if the SIR drops below a certain minimum threshold that, for the sake of simplicity, is here neglected. For the specific case of Rayleigh fading, the gain (7) for any $s \in \mathcal{B}$ admits the closed form expression (derived in the Appendix for the reader's convenience)

$$C_s(k) = \lambda_s \sum_{i \in \mathcal{B} \setminus \{s\}} \frac{\psi_{s,i}(\mathbf{a}_k)}{1 - \frac{\bar{\Gamma}_i(\mathbf{a}_k)}{\bar{\Gamma}_s(\mathbf{a}_k)}} \log_2 \frac{\bar{\Gamma}_s(\mathbf{a}_k)}{\bar{\Gamma}_i(\mathbf{a}_k)}\,, \tag{8}$$

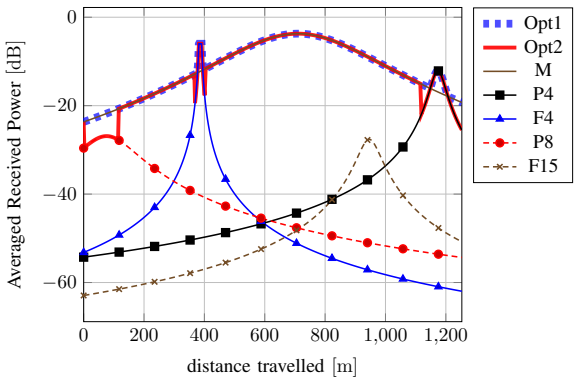

Fig. 2: Power profiles from the neighboring BSs along the UE trajectory 1, with speed $v = 40$ Km/h. The optimal policies are shown when $\lambda_M = 1$ (Opt1) and $\lambda_M = 0.2$ (Opt2).

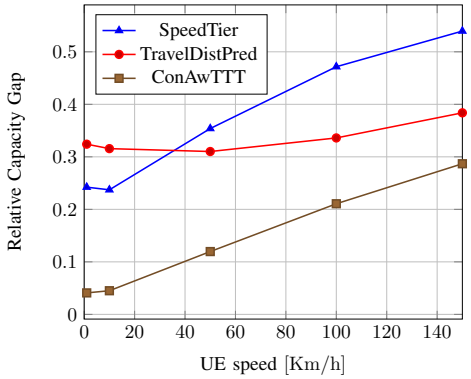

Fig. 3: Trajectory average capacity according to different HO policies.

where

$$\psi_{s,i}(\mathbf{a}_k) = \frac{1}{\prod_{j \in \mathcal{B} \setminus \{s,i\}} \left(1 - \frac{\bar{\Gamma}_j(\mathbf{a}_k)}{\bar{\Gamma}_i(\mathbf{a}_k)}\right)} \tag{9}$$

and $\bar{\Gamma}_i(\mathbf{a}_k) = \Gamma_i^{tx} g_i(\mathbf{a}_k)$ is the received power averaged over the fading process. Using (8) into (4) we can finally determine the optimal HO policy through the algorithm described in the previous section.

Figure 1 shows a test scenario, where 10 pico BSs and 20 femto BSs are randomly deployed within a macro cell coverage area of radius $R = 600$ m. The trajectory followed by the UE is shown as a solid line (traj. 1). The powers transmitted by the three-tier cells, Macro, Pico, and Femto, are $\{P_M^{tx}, P_P^{tx}, P_F^{tx}\} = \{46, 30, 24\}$ dBm, as in [14], while the pathloss coefficients are $\{\eta_M, \eta_P, \eta_F\} = \{4.5, 2.5, 2.5\}$. In this scenario, small cells are unloaded, i.e., $\lambda_P = \lambda_F = 1$, while for the macro cell we consider two cases, with $\lambda_M = 0.2$ and $\lambda_M = 1$, respectively.

Figure 2 shows the average RSRP for the macro BS M, and for the BSs that are close to the trajectory of the UE, namely the pico cells $\{\mathrm{P8}, \mathrm{P4}\}$ and femto cells $\{\mathrm{F4}, \mathrm{F15}\}$. In addition, the figure shows the average RSRP experienced by the UE when performing the optimal HO strategy in the case the macro cell is unloaded (Opt1), and heavily loaded (Opt2). As can be seen, in the second case the optimal HO strategy (thick red solid line) favors the connection to the closest (unloaded) BSs (including P8), prolonging the permanence time in the femto and pico cell with respect to the optimal strategy when the macro cell is unloaded.

B. Simulation results

To gain insight on the room available for improvement in the design of HO procedures, we have simulated some HO algorithms found in the literature in a realistic scenario with 9 macro cells placed on a grid and 75 pico cells and 145 femto cells randomly deployed at the macro cell edges. The fraction of available cell capacity for the macro, pico and femto cells are $\{\lambda_M, \lambda_P, \lambda_F\} = \{0.5, 0.8, 1\}$, respectively, while the transmitted powers and pathloss coefficients are the same as before. We generate random trajectories that cross the network area of size 3×3.6 Km^2.

The first HO algorithm considered in the comparison is the *Travel Distance Prediction* (*TravelDistPred*) [10], where the predicted distance within the cell coverage area is computed as soon as the RSRP of the target cell is higher than that of the serving cell. If the expected distance is higher than $2/3$ of the target cell radius, the HO is performed, otherwise it is avoided. The Time To Trigger (TTT) parameter, after which the HO is started, is set to $T = 10\Delta_c/v$, where v is the UE speed, and Δ_c is a fixed parameter. The second algorithm is the *Speed and Tier dependent policy* (*SpeedTier*) [11], where different TTTs are chosen according to the UE speed level (normal, medium, high) and the pair serving-target cell tiers (macro-to-macro, macro-to-small, small-to-macro, small-to-small). The third considered algorithm is the *Context-aware TTT* mechanism (*ConAwTTT*) [12], where the TTT is optimized according to UE speed and cell power profiles, while the traffic load is taken into account by properly adapting the hysteresis margin. Finally, we consider the HO performance bound derived in this paper (*Opt*).

In Figure 3 we plot the relative capacity gap G_a of the considered algorithm a with respect to the optimal policy as

$$G_a = \frac{\sum_{k \in \mathcal{K}_a} [C_{opt}(k) - C_a(k)]}{\sum_{k \in \mathcal{K}_a} C_{opt}(k)}, \tag{10}$$

where $C_{opt}(k)$ and $C_a(k)$ are the capacities at point k of the optimal policy and of one of the handover algorithms described above, while $\mathcal{K}_a$ is the set of points along the UE trajectory where $C_{opt}(k) \neq C_a(k)$. We can observe how the performance of *SpeedTier* and *TravelDistPred* intersect when varying v, while *ConAwTTT*, that takes into account different context parameters (including cell loads), achieves higher performance, closer to the optimal, for different UE speeds.

Finally, we use our mathematical model to gain insight on the performance that could be achieved by knowing the exact value of the RSRP (including the fading terms) at each point of the trajectory. To this end, we ran 1000 independent simulations of a UE crossing the macro cell along trajectory 2 in Figure 1 and, for each realization, we computed the optimal HO strategy by considering the gain function $C_s(k) = \lambda_s \log_2(1 + \gamma_s(\mathbf{a}_k, \tau_k))$. Figure 4 shows the average of the optimal performance obtained by considering the actual instantaneous gain at each point along the trajectory, and that

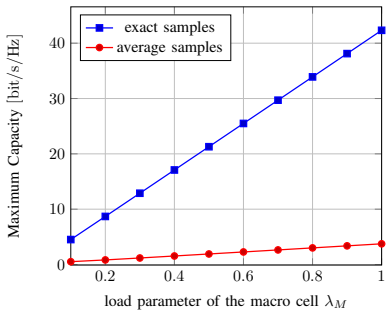

Fig. 4: Optimum capacity along the UE trajectory 2, with UE speed $v = 40$ Km/h.

obtained by considering the average gain for each point along the trajectory, i.e., using (7). We can see that these values grow linearly with the fraction of available channel capacity of the macro cell, λ_M, but the slope of the capacity curve computed from the exact samples is much higher than the other one. Hence, an accurate estimate of the fading conditions along the trajectory may potentially allow for significant performance improvements.

IV. Conclusions

In this letter, we have proposed a simple but effective mathematical framework to assess the limit of the HO performance in a given context. The model has been used to derive the HO performance bound in a sample scenario, thus providing a benchmark to assess the performance of some practical algorithms available in the literature. The model turns out to be a useful tool to understand which context parameters have a larger impact on the HO performance and, hence, can be a precious tool to design context-aware HO policies and to assess the residual margin of improvement. For example, the proposed framework can be used to design *anticipatory* HO strategies, which are based on estimates of the gain $C_s(k)$ for any k and s, rather than on the exact values.

Appendix

For the sake of simplicity, we omit the dependence on $\mathbf{a}_k$ and τ_k in the notation. The cumulative distribution function (CDF) of γ_s is computed as

$$F_{\gamma_s}(x) = \Pr\left[\gamma_s \le x\right] = \Pr\left[\alpha_s \le \frac{x}{\bar{\Gamma}_s}\left(\sum_{i\in\mathcal{B}\setminus\{s\}} \bar{\Gamma}_i \alpha_i\right)\right]$$

$$= 1 - \prod_{i\in\mathcal{B}\setminus\{s\}} \int_0^{+\infty} f_{\alpha_i}(y_i) e^{-x y_i \frac{\bar{\Gamma}_i}{\bar{\Gamma}_s}}\, \mathrm{d}y_i$$

$$= 1 - \prod_{i\in\mathcal{B}\setminus\{s\}} \int_0^{+\infty} e^{-\left(1+x\frac{\bar{\Gamma}_i}{\bar{\Gamma}_s}\right) y_i}\, \mathrm{d}y_i = 1 - \prod_{i\in\mathcal{B}\setminus\{s\}} \frac{1}{1+x\frac{\bar{\Gamma}_i}{\bar{\Gamma}_s}}.$$

The probability density function (PDF) of γ_s is given by

$$f_{\gamma_s}(x) = \frac{\mathrm{d}}{\mathrm{d}x} F_{\gamma_s}(x) = \frac{\sum_{i\in\mathcal{B}\setminus\{s\}} \frac{\bar{\Gamma}_i}{\bar{\Gamma}_s} \prod_{j\in\mathcal{B}\setminus\{s,i\}} \left(1+x\frac{\bar{\Gamma}_j}{\bar{\Gamma}_s}\right)}{\prod_{i\in\mathcal{B}\setminus\{s\}} \left(1+x\frac{\bar{\Gamma}_i}{\bar{\Gamma}_s}\right)^2}$$

$$= \sum_{i\in\mathcal{B}\setminus\{s\}} \left(\frac{\bar{\Gamma}_i}{\bar{\Gamma}_s}\right)^N \frac{1}{\prod_{j\in\mathcal{B}\setminus\{s,i\}} \left(\frac{\bar{\Gamma}_i}{\bar{\Gamma}_s} - \frac{\bar{\Gamma}_j}{\bar{\Gamma}_s}\right)} \frac{1}{\left(1+x\frac{\bar{\Gamma}_i}{\bar{\Gamma}_s}\right)^2}$$

$$= \sum_{i\in\mathcal{B}\setminus\{s\}} \underbrace{\frac{1}{\prod_{j\in\mathcal{B}\setminus\{s,i\}} \left(1-\frac{\bar{\Gamma}_j}{\bar{\Gamma}_i}\right)}}_{\psi_{s,i}} \frac{\frac{\bar{\Gamma}_i}{\bar{\Gamma}_s}}{\left(1+x\frac{\bar{\Gamma}_i}{\bar{\Gamma}_s}\right)^2}.$$

Finally, the expectation in (7) is computed as

$$\mathbb{E}\left[\log_2\left(1+\gamma_s\right)\right] = \int_0^{+\infty} f_{\gamma_s}(x) \log_2(1+x)\, \mathrm{d}x$$

$$= \log_2 e \int_0^{+\infty} \sum_{i\in\mathcal{B}\setminus\{s\}} \psi_{s,i} \frac{\frac{\bar{\Gamma}_i}{\bar{\Gamma}_s}}{\left(1+x\frac{\bar{\Gamma}_i}{\bar{\Gamma}_s}\right)^2} \ln(1+x)\, \mathrm{d}x$$

$$= \log_2 e \sum_{i\in\mathcal{B}\setminus\{s\}} \frac{\psi_{s,i}}{1-\frac{\bar{\Gamma}_i}{\bar{\Gamma}_s}} \ln\left(\frac{1+x}{1+x\frac{\bar{\Gamma}_i}{\bar{\Gamma}_s}}\right)\Bigg|_0^{+\infty}$$

$$= \sum_{i\in\mathcal{B}\setminus\{s\}} \frac{\psi_{s,i}}{1-\frac{\bar{\Gamma}_i}{\bar{\Gamma}_s}} \log_2 \frac{\bar{\Gamma}_s}{\bar{\Gamma}_i}.$$

References

[1] T. Zahir, K. Arshad, A. Nakata, K. Moessner, "Interference Management in Femtocells," *IEEE Communications Surveys & Tutorials,* vol. 15, no. 1, pp. 293–311, First Quarter 2013.

[2] X. Lin, R. K. Ganti, P. Fleming, J. G. Andrews, "Towards Understanding the Fundamentals of Mobility in Cellular Networks," *IEEE Transactions on Wireless Communications,* vol. 12, no. 4, April 2013.

[3] Y. Song, P.-Y. Kong, Y. Han, "Power-Optimized Vertical Handover Scheme for Heterogeneous Wireless Networks," *IEEE Communications Letters,* vol. 18, no. 2, pp. 277–280, February 2014.

[4] D. Xenakis, N. Passas, L. Merakos, C. Verikoukis, "Energy-efficient and interference-aware handover decision for the LTE-Advanced femtocell network," *IEEE International Conference on Communications (ICC),* pp. 2464–2468, June 2013.

[5] H. Zhou, D. Hu, S. Mao, P. Agrawal, S. A. Reddy, "Cell association and handover management in femtocell networks," *IEEE Wireless Communications and Networking Conference (WCNC),* pp. 661–666, April 2013.

[6] N. Zia, S. S. Mwanje, A. Mitschele-Thiel, "A policy based conflict resolution mechanism for MLB and MRO in LTE self-optimizing networks," *IEEE Symposium on Computers and Communication (ISCC),* pp. 1–6, June 2014.

[7] Q. Shen, J. Liu, Z. Huang, X. Gan, Z. Zhang, D. Chen, "Adaptive double thresholds handover mechanism in small cell LTE-A network," *6th International Conference on Wireless Communications and Signal Processing (WCSP),* pp. 1–6, October 2014.

[8] Y. Li, B. Cao, C. Wang, "Handover schemes in heterogeneous LTE networks: challenges and opportunities," *IEEE Wireless Communications,* vol. 23, no. 2, pp. 112–117, April 2016.

[9] D. Xenakis, N. Passas, L. Merakos, C. Verikoukis, "Mobility Management for Femtocells in LTE-Advanced: Key Aspects and Survey of Handover Decision Algorithms," *IEEE Communications Surveys & Tutorials,* vol. 16, no. 1, pp. 64–91, First Quarter 2014.

[10] X. Yan, M. Nallasamy, Y. A. Sekercioglu, "A Traveling Distance Prediction Based Method to Minimize Unnecessary Handovers from Cellular Networks to WLANs," *IEEE Communications Letters,* vol. 12, no. 1, pp. 14–16, January 2008.

[11] S. Barbera, P. H. Michaelsen, M. Saily, K. Pedersen, "Improved mobility performance in LTE co-channel HetNets through speed differentiated enhancements," *IEEE Globecom*, pp. 426–430, December 2012.

[12] F. Guidolin, I. Pappalardo, A. Zanella, M. Zorzi, "Context-Aware Handover Policies in HetNets," *IEEE Transactions on Wireless Communications*, vol. 15, no. 3, pp. 1895-1906, March 2016.

[13] T. S. Rappaport, *Wireless Communications: Principles & Practice, 2nd Edition,* Prentice Hall, 2002.

[14] R. Tanbourgi, S. Singh, J. G. Andrews, F. K. Jondral, "Analysis of Non-Coherent Joint-Transmission Cooperation in Heterogeneous Cellular Networks," *IEEE International Conference on Communications (ICC),* June 2014.